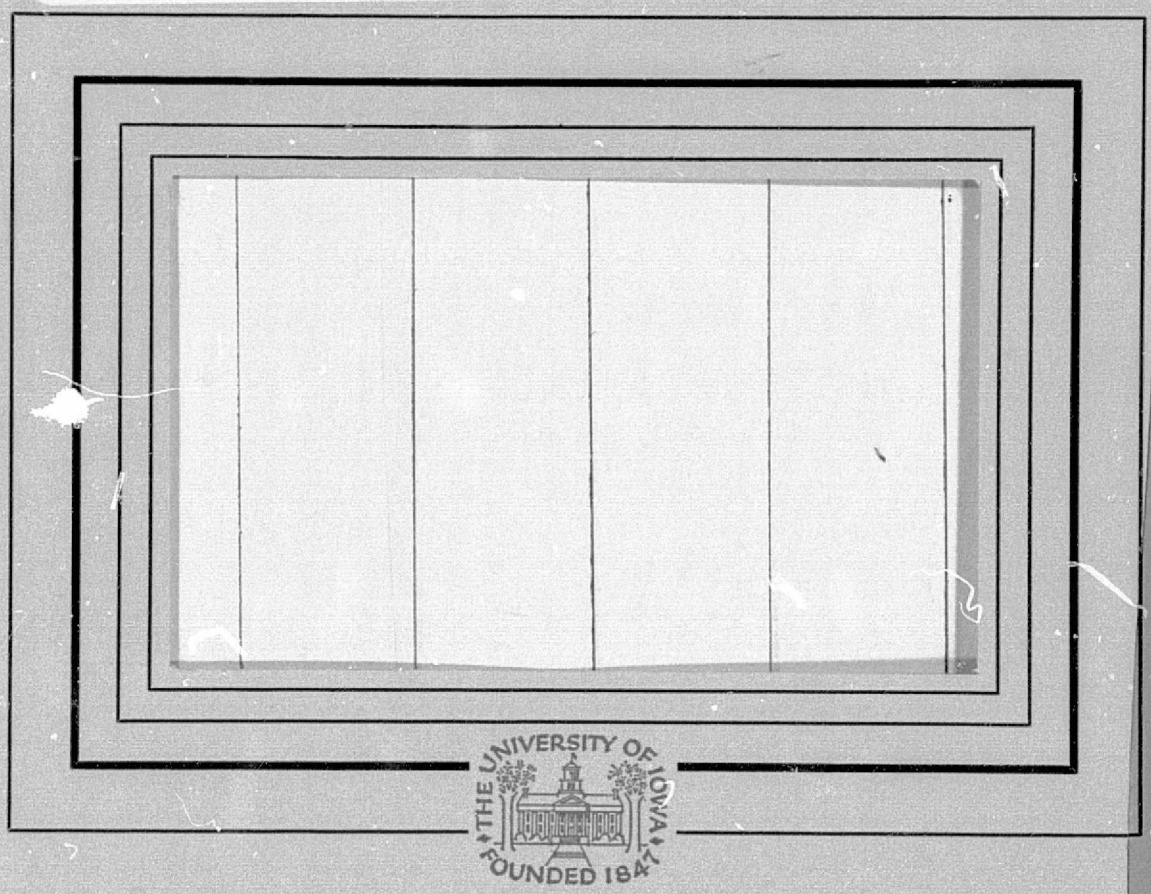

"Research was supported in part by the Office of Naval Research under Contract N00014-76-C-0016."

Department of Physics and Astronomy

THE UNIVERSITY OF IOWA

Iowa City, Iowa 52242

DIRECTION-FINDING MEASUREMENTS OF TYPE III RADIO BURSTS OUT OF THE ECLIPTIC PLANE*†

By

Mark M. Baumback, William S. Kurth,

and Donald A. Gurnett

Department of Physics and Astronomy
The University of Iowa
Iowa City, Iowa 52242

December 1975

This work was supported in part by the National Aeronautics and Space Administration under Contracts NAS1-13129 and NAS5-11431 and Grant NGL-16-001-043 and by the Office of Naval Research under Grant N00014-76-C-0016.

*Submitted to Solar Physics

†Presented at Workshop on "Mechanisms for Solar Type III Radio Bursts", Berkeley, California, May 8-9, 1975.

UNCLASSIFIED
SECURITY CLASSIFICATION OF THIS PAGE (When Data Entered)

REPORT DOCUMENTATION PAGE

READ INSTRUCTIONS BEFORE COMPLETING FORM

1. REPORT NUMBER: U. of Iowa 75-45
2. GOVT ACCESSION NO.:
3. RECIPIENT'S CATALOG NUMBER:

4. TITLE (and Subtitle): DIRECTION-FINDING MEASURMENTS OF TYPE III RADIO BURSTS OUT OF THE ECLIPTIC PLANE
5. TYPE OF REPORT & PERIOD COVERED: Progress December 1975
6. PERFORMING ORG. REPORT NUMBER:

7. AUTHOR(s): Mark M. Baumback, William S. Kurth, and Donald A. Gurnett

8. CONTRACT OR GRANT NUMBER(s): N00014-76-C-0016

9. PERFORMING ORGANIZATION NAME AND ADDRESS: Department of Physics and Astronomy
The University of Iowa
Iowa City, Iowa 52242

10. PROGRAM ELEMENT, PROJECT, TASK AREA & WORK UNIT NUMBERS:

11. CONTROLLING OFFICE NAME AND ADDRESS: Office of Naval Research
Arlington, Virginia 22217

12. REPORT DATE: December 1975
13. NUMBER OF PAGES: 49

14. MONITORING AGENCY NAME & ADDRESS(if different from Controlling Office):

15. SECURITY CLASS. (of this report): UNCLASSIFIED
15a. DECLASSIFICATION/DOWNGRADING SCHEDULE:

16. DISTRIBUTION STATEMENT (of this Report)

Approved for public release; distribution is unlimited.

17. DISTRIBUTION STATEMENT (of the abstract entered in Block 20, if different from Report)

18. SUPPLEMENTARY NOTES

Submitted to Solar Physics, December 1975

19. KEY WORDS (Continue on reverse side if necessary and identify by block number)

Type III Bursts
Radio-Direction Finding
Out of the Ecliptic Plane

20. ABSTRACT (Continue on reverse side if necessary and identify by block number)

[See page following.]

DD FORM 1 JAN 73 1473 EDITION OF 1 NOV 65 IS OBSOLETE
S/N 0102-014-6601

UNCLASSIFIED
SECURITY CLASSIFICATION OF THIS PAGE (When Data Entered)

ABSTRACT

Direction-finding measurements with the plasma wave experiments on the HAWKEYE 1 and IMP 8 satellites are used to find the source locations of type III solar radio bursts in heliocentric latitude and longitude in a frequency range from 31.1 kHz to 500 kHz. IMP 8 has its spin axis perpendicular to the ecliptic plane; hence, by analyzing the spin modulation of the received signals the location of the type III burst projected into the ecliptic plane can be found. HAWKEYE 1 has its spin axis nearly parallel to the ecliptic plane; hence, the location of the source out of the ecliptic plane may also be determined. Using an empirical model for the emission frequency as a function of radial distance from the sun the three-dimensional trajectory of the type III radio source can be determined from direction-finding measurements at different frequencies. Since the electrons which produce these radio emissions follow the magnetic field lines from the sun these measurements provide information on the three-dimensional structure of the magnetic field in the solar wind. The source locations projected into the ecliptic plane follow an Archimedian spiral. Perpendicular to the ecliptic plane the source locations usually follow a constant heliocentric latitude. When the best fit magnetic field line through the source locations is extrapolated back to the sun this field line usually originates within a few degrees from the solar flare which produced the radio burst. With direction-finding measurements of this type it is also

possible to determine the source size from the modulation factor of the received signals. For a type III event on June 8, 1974, the half angle source size was measured to be ~ 60° at 500 kHz and ~ 40° at 56.2 kHz as viewed from the sun.

I. INTRODUCTION

Broadband radio emissions of solar origin characterized by a rapid decrease in frequency with increasing time were first reported by Wild and McCready (1950) and designated type III radio bursts. These first observations of type III bursts were made in the frequency range from 70 to 130 MHz. In addition to being characterized by a rapid frequency drift, type III bursts have lifetimes which increase with decreasing frequency and have shorter rise times than decay times. The amplitude of the bursts during the decay is proportional to e^{-kt} (Wild 1950), where k is the decay constant and t is time. For a general review of ground based type III radio burst observations see Kundu (1965).

Wild et al. (1954) speculated that the rapid frequency drift is caused by charged particles moving outward through the solar corona emitting electromagnetic radiation at a frequency characteristic of the solar wind. Solar flare electrons with energies of ~ 40 keV were first observed in the interplanetary medium and identified to be of solar origin by Van Allen and Krimigis (1965). A high correlation between the onset of solar flare electrons in the energy range of 1 to 100 keV and type III emission near 1.0 AU indicates that these electrons generate the type III bursts (Lin 1970, Alvarez et al. 1972, Frank and Gurnett 1972, Lin et al. 1973, Alvarez et al. 1975, Gurnett and Frank 1975).

Measurements of the frequency drift rates of type III bursts provide information on the solar wind density, if the frequency of emission as a function of heliocentric radial distance is assumed to be related to the local plasma frequency. The velocity of the exciter electrons may also be determined from the frequency drift rates. Exciter velocities ranging from 0.2 to 0.8 times the velocity of light with an average velocity of 0.45 c were calculated for frequencies between 60 and 45 MHz (Wild et al. 1959). The average exciter velocity calculated from measurements by the RAE 1 satellite for frequencies between 3.7 MHz and 2.8 MHz was 0.38 c (Fainberg and Stone 1970). Other drift rate measurements give similar results (Hartz 1964, 1969; Alexander et al. 1969; Haddock and Graedel 1970; Fainberg and Stone 1971). These drift rate measurements give electron velocities that are in agreement with the energy range of the solar electrons observed in the interplanetary medium by the satellite experiments.

Ginzberg and Zhelezniakov (1958) suggested that type III bursts are generated by a coherent Cerenkov process. The energetic particles generate plasma waves at a frequency near the local plasma frequency by a two-stream instability. Then the plasma waves scatter off ion density inhomogeneities to produce electromagnetic radiation near the plasma frequency and also scatter off other plasma waves to produce radiation near the second harmonic. The theory has since been revised but the process is basically the same (Smith 1970, 1974).

Models of the density of the solar wind can be used to determine the radial distances from the sun at which type III bursts radiate at different frequencies. Kaiser's (1975) study of the solar

elongation of type III bursts indicates that the density of the solar wind from approximately 0.1 AU to 1.0 AU varies as $R^{-\gamma}$ where $2 \leq \gamma \leq 3$. Measurements of several thousand events were used to formulate the RAE emission level scale (Fainberg et al. 1972, Fainberg and Stone 1974). The RAE emission level scale relates the frequency of emission of a type III burst to the radial distance of the burst from the sun. A solar wind density model can be computed from the RAE emission level scale if it is assumed that the radiation occurs at the fundamental or second harmonic of the plasma frequency. Initially the radiation was assumed to be at the fundamental of the plasma frequency (Fainberg et al. 1972). The solar wind density models formulated from the analysis of type III bursts assuming emission at the fundamental of the plasma frequency usually disagreed with the observed plasma densities at 1.0 AU (Newkirk 1967). Evidence now exists that radiation is predominantly at the second harmonic for low frequencies (Fainberg et al. 1972, Fainberg and Stone 1974, Lin et al. 1973, Haddock and Alvarez 1973, Alvarez et al. 1975, Kaiser 1975). The assumption of second harmonic emission brings densities calculated from the RAE emission level scale to better agreement with solar wind density measurements at 1.0 AU. For a model of the solar wind plasma density this paper uses the RAE emission level scale with the assumption of second harmonic emission. For a review of density measurements see Newkirk (1967).

Since the electrons that generate type III bursts travel along the solar magnetic field lines, information can be obtained about the structure of the interplanetary magnetic field by analyzing the direction of arrival of a type III burst as a function of frequency. The source location of the type III burst can be determined from the direction-finding measurements and the radial distance of the emission from the sun can be computed from a model of the solar wind density. The source location of the burst as a function of frequency, and hence radial distance, trace the magnetic field out from the sun.

The first direction-finding measurements of type III bursts were made by Slysh (1967) using spin modulation and lunar occultations of the Luna 11 and 12 satellites to determine the source locations. Direction-finding measurements on the IMP 6 spacecraft confirmed that the type III emission regions as a function of frequency, and hence the electrons generating the type III bursts, follow the Archimedean spiral structure of the solar magnetic field (Lin et al. 1973, Fainberg et al. 1972, Fainberg and Stone 1974, Stone 1974).

Up to the present time direction-finding measurements of type III radio bursts have only provided one coordinate, in the plane of rotation of the antenna, of the direction of arrival. These one-dimensional measurements therefore only give a projection of the source location and do not provide a unique determination of the trajectory of the radio burst. Measurements of the source size from the spin modulation are similarly ambiguous for such one-dimensional measurements since the modulation of the received signal is also a function of the unknown elevation angle of the source above the plane of rotation of the antenna.

The purpose of this paper is to present a series of two-dimensional direction-finding measurements of type III radio bursts using spin modulation measurements from two satellites (IMP 8 and HAWKEYE 1) which have their spin axes nearly perpendicular to each other. Simultaneous direction-finding measurements from these satellites provide a unique determination of the direction of arrival (along a line) and the angular size of the source. This two-dimensional direction-finding technique is used, together with a model for the solar wind plasma density, to provide determinations of type III source locations out of the ecliptic plane and information on the three-dimensional structure of the solar magnetic field at radial distances of 0.2 to 1.0 AU from the sun.

II. DESCRIPTION OF INSTRUMENTATION

Data from two satellites, IMP 8 and HAWKEYE 1, are used in the direction-finding analysis. The three events analyzed occurred during June and July, 1974. All of the data presented in this paper were taken while the satellites were in the solar wind. Therefore, it was possible to analyze events down to frequencies near the solar wind plasma frequency, which is typically about 25 kHz at 1.0 AU.

The IMP 8 spacecraft was launched into earth orbit from the Eastern Test Range on October 26, 1973. The orbit is slightly eccentric with initial perigee and apogee geocentric radial distances of 147,434 km and 295,054 km, respectively, inclination of 28.6°, and period of 11.98 days. The spacecraft is spin stabilized with its spin axis oriented very nearly perpendicular to the ecliptic plane with a spin period of about 2.59 sec.

The University of Iowa plasma wave experiment on IMP 8 measures the average electric field intensity in a frequency range from 40 Hz to 2 MHz and the average magnetic field intensity from 40 Hz to 1.78 kHz. The electric field receiver is connected to a dipole antenna with a nominal tip-to-tip length of 121.8 m extended perpendicular to the spin axis, and the magnetic field receiver is connected to a triaxial search coil magnetometer. Electric field spectral measurements are made in 15 fixed frequency channels extending from 40 Hz to 178 kHz and in one channel with selectable frequency. The selectable frequency channel may be tuned to measure the average electric

field intensity at 31.1 kHz, 125 kHz, 500 kHz, or 2 MHz with a bandwidth of ± 1.0 kHz.

The HAWKEYE 1 spacecraft was launched into polar earth orbit on June 3, 1974 from the Western Test Range. The orbit is highly eccentric with initial perigee and apogee geocentric radial distances of 6847 km and 130,856 km, respectively, inclination of 89.79°, and period of 49.94 hours. The initial argument of perigee is 274.6°; thus, apogee is almost directly over the north pole. The spacecraft is spin stabilized with a spin period of about 11.0 sec. The spin axis lies in the plane of the orbit and is nearly parallel to the equatorial plane with a right ascension of 300.7° and declination of 6.8°.

The HAWKEYE 1 plasma wave experiment is similar to the IMP 8 plasma wave experiment. The electric field receiver is connected to a dipole antenna with a nominal tip-to-tip length of 42.45 m extended perpendicular to the spin axis. The magnetic field receiver is connected to a search coil magnetometer that is oriented parallel to the spin axis. Electric field spectral measurements are made in 16 fixed frequency channels extending from 1.78 Hz to 178 kHz, and magnetic field spectral measurements are made in 8 frequency channels extending from 1.78 Hz to 5.62 kHz.

III. DIRECTION-FINDING TECHNIQUE

A. Calculation of the Direction of Arrival

The amplitude of the detected signals from each satellite has a modulation caused by the rotation of the electric dipole antenna. The angular position of the null in the modulation pattern can be used to determine a component of the source direction. The null in the modulation pattern occurs when the antenna is most nearly parallel to the wave propagation vector, and the maximum occurs when the antenna axis is perpendicular to the propagation vector. The depth of the null is determined by the size of the source and the elevation angle, α, between the plane of rotation of the antenna and the source direction. As α increases or as the source size increases the depth of the null decreases.

For both HAWKEYE 1 and IMP 8 the data sampling intervals are comparable to the spin period; thus, many rotations of the satellite are required to obtain a uniform angular distribution of samples through 360°. The time period necessary to collect a complete set of samples through 360° will be referred to as a sampling cycle.

The direction-finding routines used for analysis normalize the data to reduce the effects of amplitude changes that take place in a time interval that is long compared to the spin period. This normalization is performed by subtracting the average of all samples

in the sampling cycle from each of the individual samples. Since the samples are proportional to the logarithm of the electric field intensity the normalization process is equivalent to dividing each sample by the geometric average intensity during the sampling cycle.

To determine the null direction, δ, data is accumulated over the duration of the type III event at each frequency and is then fit by the method of least squares to the theoretical modulation envelope given by

$$\left(\frac{E}{E_o}\right)^2 = \left(1 - \frac{m}{2}\right) - \frac{m}{2} \cos\left[2(\delta_y - \delta)\right] \quad , \tag{1}$$

where E/E_o is the normalized intensity and δ_y is the orientation angle of the electric antenna axis in the plane of rotation of the antenna. The null direction, δ, is the direction to the centroid of the source projected onto the spin plane of the antenna. The modulation factor, m, provides a quantitative measure of the null depth: m is zero for no spin modulation, and m is one for the maximum modulation. The null direction computed represents the least squares fit δ over the duration of the event. Each sample receives an equal weighting in the analysis. Since the dipole pattern is assumed to be symmetric, the data from $90° \leq \delta_y < 270°$ is shifted into the range from $-90° \leq \delta_y < 90°$ by subtracting 180°.

Another direction-finding routine used for IMP 8 computes the null direction averaged over 10 minute intervals, rather than the average null direction for the entire event. For this routine samples from

the current sampling cycle receive a weight of 1 while samples from previous sampling cycles are multiplied by a weighting factor that decreases exponentially for earlier times. The exponential weighting factors make it possible to compute δ averaged over a shorter pre-selected time interval in order to study changes in the direction of arrival during an event.

B. Geometry in the Analysis

The null direction computed from each satellite locates a plane in which the source must lie. The source lies along the intersection of the source planes determined by the two satellites. Figure 1 shows the geometry of the source planes and the angles and vectors used for the computation of the source location. The spin plane is the plane in which the antenna rotates. The spin axis, $\vec{S}$, is perpendicular to the spin plane. The source plane is the plane in which both the spin axis of the satellite and the source lie. The angle between the satellite-sun line projected into the spin plane and the intersection between the spin plane and the source plane is δ. Normals to both source planes are constructed. $\hat{n}_1$ is normal to IMP 8's source plane and $\hat{n}_2$ is normal to HAWKEYE 1's source plane. The source location vector is given by $\hat{n}_1 \times \hat{n}_2$. There is, however, a 180° ambiguity in the source location. At high frequencies this ambiguity is decided by assuming that the source is in the direction toward the sun. At lower frequencies, where the source could be located at radial distances beyond 1.0 AU if the emission is at the second harmonic of the plasma frequency, the ambiguity is decided by requiring the source position to be in agreement

with an extrapolation of the measurements at higher frequencies. The source direction computed from $\hat{n}_1 \times \hat{n}_2$, after deciding the ambiguity, is given in geocentric solar ecliptic coordinates, λ_{GSE} and φ_{GSE}. The angle λ_{GSE} is the geocentric solar ecliptic latitude of the source, measured positive northward from the ecliptic plane. The angle φ_{GSE} is the solar ecliptic longitude of the source, measured positive counterclockwise from the sun-satellite line as viewed from the north ecliptic pole. Since the IMP 8 spin axis is perpendicular to the ecliptic plane the null angle δ, which is referenced to the sun direction, is identical to the geocentric solar ecliptic longitude of the source.

IV. CHARACTERISTICS OF TYPE III BURSTS OBSERVED BY IMP 8 AND HAWKEYE 1

At frequencies below 1 MHz, type III bursts have several readily observed features. Type III bursts are characterized by a rapid decrease in frequency with increasing time. The modulation factor of the burst varies with frequency and time. The direction of arrival is also observed to vary in time for any one frequency. Figure 2 shows a type III event observed simultaneously by both IMP 8 and HAWKEYE 1. This figure is a plot of the logarithm of the electric field intensity measured by the plasma wave experiments on board the two satellites. The data from seven frequency channels of each experiment are displayed as a function of time. Notice that in addition to a type III event, other naturally occurring radio signals such as auroral kilometric radiation and magnetosheath electrostatic noise are observed. The characteristic frequency drift is evident in the type III event shown in Figure 2.

The modulation factor observed at a particular frequency is usually greater near the start of the burst than near the end of the burst. The modulation factor also decreases with decreasing frequency. At 500 kHz the modulation is usually greater than 0.80 while at frequencies on the order of the local plasma frequency at 1.0 AU the modulation disappears completely. Figure 3 shows data from the

100 kHz channel of the IMP 8 experiment. In the top panel the logarithm of the electric field intensity is plotted as a function of time. The modulation of the received electric field intensity caused by the rotation of the dipole antenna is seen as a periodic amplitude fluctuation with a periodicity of about 100 sec. The bottom panel of Figure 3 displays the modulation factor calculated from Eq. (1) as a function of time. The modulation factor at the start of the burst is about 0.65 while near the end of the burst the modulation factor is about 0.25.

At a particular frequency the direction of arrival changes systematically during the duration of the burst, usually starting near the sun and deviating away from the sun later in the event. The direction of arrival usually varies over a wider range at the lower frequencies. At 500 kHz there is a shift in φ_{GSE} of the source of about 10°, while at 56.2 kHz the φ_{GSE} shifts by as much as 60°. An example of this angle drift at 100 kHz is shown in the center panel of Figure 3. φ_{GSE} is initially near 0° (in the direction of the sun), but then changes to approximately 45° at the end of the event. To compute the source locations for the events analyzed in this paper, the direction of arrival is the least squares fit δ computed over the duration of the event.

V. PLASMA DENSITY AND SOLAR MAGNETIC FIELD MODELS

Models of the solar wind density and the solar magnetic field are necessary to determine the source locations of the type III burst in three-dimensions. Since data from only two satellites are used in the analysis, only two components of the source locations can be determined. A model of the solar wind plasma density provides the information required to determine the third component of the source locations.

A. RAE Emission Level Scale

The frequency of emission of type III bursts is a function of solar wind density; therefore, if a density scale of the solar wind as a function of heliocentric radial distance is assumed, it is possible to calculate the distance from the sun to the type III burst emission region. The RAE emission level scale (Fainberg and Stone 1970, 1974; Fainberg et al. 1972) gives the frequency of emission as a function of heliocentric radial distance, independent of any assumption of the solar wind density. A density scale for the solar wind can be computed by assuming that the frequency of emission is at either the plasma frequency or at a harmonic of the plasma frequency.

The density scale shown in Figure 4 is based on the RAE emission level scale and assumes emission at the second harmonic of the plasma frequency.

Since the RAE emission level scale is an average of many thousands of bursts, it is desirable on an individual basis to adjust the RAE emission level scale so that the density scale agrees with the plasma density measured at 1.0 AU in the solar wind. When the trajectory of the exciter electrons passes near the earth and in situ measurements of the solar wind density are available, the RAE emission level scale is adjusted to agree with the density measurements.

B. Solar Magnetic Field Line Configuration in the Ecliptic Plane

In the interplanetary medium the magnetic fields are constrained to move with the solar wind plasma flow. For the simplest model, the solar wind plasma flows radially out of the sun at a constant velocity of approximately 400 km/sec^{-1}. Since the sun is rotating the resulting magnetic field projected into the ecliptic plane corresponds to an Archimedean spiral (Parker 1963, 1964, 1965). Measurements in the ecliptic plane confirm the general spiral structure of the magnetic field (Schatten et al. 1968, and review by Schatten 1972); however, the magnetic field is usually distorted from a perfect spiral configuration. For example, changes in the velocity of the solar wind will produce kinks in the spirals. Other distortions may be caused by variations in the magnetic field near the sun and by

magnetic field loops in which the field lines near the sun reconnect back to the sun (Schatten 1972).

C. Solar Magnetic Field Line Structure in the Meridian Plane

No direct measurements have been made of the solar magnetic field configuration out of the ecliptic plane, in the interplanetary medium. The structure of the solar magnetic field may be deduced by indirect measurements, such as the analysis of type III bursts, because the trajectory of the electrons that generate type III bursts is along the solar magnetic field lines.

The simplest model of the solar magnetic field out of the ecliptic plane is the constant latitude model shown in Figure 5, which corresponds to a uniform radial flow of the solar wind plasma away from the sun. Projected into the ecliptic plane the field lines are Archimedean spirals, while in a meridian plane the magnetic field lines are at a constant latitude. The constant latitude model corresponds to Archimedean spirals wound on cones of constant heliocentric latitudes.

The structure of the solar corona photographed during solar eclipses indicates that high latitude polar fields may extend to low latitudes at 1.0 AU (Schatten 1972). The convergent field line model shown in Figure 5 is suggested by these observations. For this model the solar magnetic field projected into the ecliptic plane follows the Archimedean spiral but in the meridian plane the magnetic

field lines extend to lower heliocentric latitudes with increasing radial distances.

Magnetic field measurements near 1.0 AU show a consistent skewing of the magnetic field away from the equatorial plane (Coleman and Rosenberg 1971, Rosenberg and Winge 1974). Such skewing may be caused by magnetic field diffusion in the interplanetary medium (Schatten 1972). Stream interactions may contribute to an azimuthal velocity component in the solar wind or to a net divergence of mass and magnetic flux away from the equatorial plane (Suess et al. 1975). The divergence of the magnetic field away from the equator could also be caused by magnetic pressure. The magnetic field spiral angle and, therefore, the magnetic pressure changes with heliocentric latitude. The magnetic pressure is greatest near the equator, causing mass and magnetic flux to be carried away from the equatorial plane (Suess 1974, Suess and Nerney 1975). These observations suggest the divergent field line model shown in Figure 5. The magnetic field projected into the ecliptic plane follows an Archimedean spiral, but in the meridian plane the magnetic field lines extend to higher heliocentric latitudes with increasing radial distances.

Coronal photographs and in situ measurements of the solar magnetic field each suggest different models of the solar magnetic field. It is the purpose of this paper to test these various solar magnetic field models.

VI. ANALYSIS OF EVENTS

Twenty type III events were initially chosen from the first 43 orbits of HAWKEYE 1 and from the same time period for IMP 8 (June through August, 1974). Of the initial 20 events only three events were analyzed in detail, while the others were thrown out for various reasons. Some events were multiple events originating from different regions of the sun. Other events did not have adequate coverage with both satellites and for some events the modulation factor was too low to determine the direction of arrival accurately.

A. Direction of Arrival Analysis

Figures 6, 7, and 8 show the source locations for the three events that were analyzed as determined by simultaneous direction-finding measurements from HAWKEYE 1 and IMP 8 data, the RAE emission level scale, and the assumption of emission at the second harmonic of the plasma frequency. Since the trajectory of the burst in the first event (shown in Figure 6) was near the earth the RAE emission level scale was adjusted so that the density scale agreed with *in situ* measurements of the solar wind density at 1.0 AU (M. Montgomery, personal communication, 1975). The RAE emission level scale was not adjusted for the last two events (shown in Figures 7 and 8) because the trajectory of the bursts were so far from the earth that the densities measured by IMP 8 could not be considered representative of the density at 1.0 AU along the trajectories of the bursts.

For each event an Archimedean spiral is fit through the source locations projected into the ecliptic plane. Since HAWKEYE 1's spin plane is not oriented exactly perpendicular to the ecliptic plane it is necessary to know the φ_{GSE} coordinate of the source position before λ_{GSE} can be determined. If φ_{GSE} could not be determined from the IMP 8 data it was computed from the Archimedean spiral fit through the available data points. Errors in λ_{GSE} caused by computing φ_{GSE} are estimated to be smaller than 3°. The GSE latitudes (λ_{GSE}) and GSE longitudes (φ_{GSE}) for the three events are summarized in Table I. Any λ_{GSE} in Table I that required the Archimedean spiral fit to compute φ_{GSE} is indicated by an asterisk.

The upper left-hand panel in Figures 6, 7, and 8 shows the source locations projected into the ecliptic plane and the best fit Archimedean spiral through the source locations. A solar wind velocity of 400 km sec^{-1} was used to construct the Archimedean spiral. The lower left-hand panel shows the Geocentric Solar Ecliptic longitude (φ_{GSE}) of the least squares fit Archimedean spiral as viewed from earth as a function of heliocentric radial distance. The experimental values of φ_{GSE} are also shown. The upper right-hand panel shows the heliocentric latitude of the source location as a function of frequency, and the least squares fit magnetic field line using the constant latitude model. The lower right-hand panel shows the geocentric solar ecliptic latitudes (λ_{GSE}) of the best fit field line as a function of heliocentric radial distance and the observed λ_{GSE} of the source locations.

The most probable flare location for each event is found by extrapolating the magnetic field line obtained from the constant latitude model back to the sun. For the three events analyzed the differences between the actual flare location (NOAA 1974, 1975) and the flare location computed from the least squares fit magnetic field line are in all cases less than 9° in heliocentric latitude and less than 12° in heliocentric longitude. The first event, shown in Figure 6, deviates significantly from the constant latitude model of the magnetic field. The heliocentric latitude of the 100 kHz, 56.2 kHz, and 42.2 kHz source locations suggest that the convergent field line model may best represent this event. The other two events (Figures 7 and 8) are best represented by the constant latitude model.

B. Source Size of Type III Bursts

The modulation factor of the emissions can be used to estimate the source size when the elevation angle, α, of the source is known. For this analysis the half angle source size is defined as the angle between a line from the observer to the centroid of the source and a line from the observer to the edge of the source. The source is modeled as a thin, flat disk from which radiation is emitted with a uniform intensity. For a given source size the solid angle of the disk remains constant for all elevation angles, α. The calculated source sizes represent the longitudinal extent of the source.

Figure 9 shows the source sizes of the June 8 event as viewed from the earth. As would be expected, the source size increases as

the emission region nears the earth. Figure 10 shows the source sizes for the same event, but, as viewed from the sun. The source sizes for the 500 kHz, 178 kHz, and 100 kHz remain relatively constant with increasing radial distance; however, they are approximately twice as large as the 60° full width half maximum values that Lin (1974) and Alvarez et al. (1975) report for particle fluxes associated with type III events. Scattering of the radio emissions may be responsible for the large apparent source sizes.

VII. DISCUSSION

Two of the three type III events presented in this paper are in agreement with the constant latitude model of the solar magnetic field. One event (June 8) is more consistent with the convergent field line model. However, the convergent field line model contradicts some measurements of the skewing of the magnetic field away from the equatorial plane which have been made at 1.0 AU (Coleman and Rosenberg 1971, Rosenberg and Winge 1974). None of the events presented indicates that the magnetic field lines cross the ecliptic plane or that the divergent field line model is valid. Additional evidence supporting the constant latitude model is that the predicted flare locations are in good agreement with the observed flare locations.

Three features of type III bursts presented in this study are of special interest. The source sizes measured are a factor of two larger than the angular sizes of the solar electron emissions from a flare reported by Lin (1974) and Alvarez et al. (1975). The modulation factor tends to be largest near the beginning of an event, and the direction of arrival of the radiation varies systemmatically during the event, usually starting near the sun and deviating away from the sun later in the event.

One possible explanation of all three features is a combination of emission at both the fundamental and the second harmonic of the plasma frequency. If a stream of particles generating a type III burst

moves outward from the sun and generates emission at both the fundamental and second harmonic of the plasma frequency the fundamental emission would be seen first in a particular frequency channel, followed by the second harmonic emission. The shift in the direction of arrival of the radiation could be explained by emission containing both fundamental and second harmonic radiation. The fundamental emission region would be closer to the sun than the second harmonic emission region; therefore, for most Archimedean spiral positions the direction of the source would start near the sun and drift away from the sun in a systematic way, as is observed in many cases. A larger angle shift would be seen in the lower frequency channels because the source locations are closer to the earth. The source size would be smaller for fundamental emission because the size of the source region grows larger with increasing radial distance from the sun, and the source region for fundamental emission is usually farther from the earth than the second harmonic source region; explaining the higher observed modulation factor near the start of the event. With simultaneous emission of both fundamental and second harmonic radiation the apparent source sizes would be much larger than the individual source sizes for fundamental and second harmonic emission.

There are other possible explanations for the systematic drifts in source location and variations in the modulation factor which should also be considered. Irregularities in the solar wind density could cause different regions to radiate at the same frequency at different times thus causing the observed changes in the angular

position of the source. If the radiation is not circular or randomly polarized, changes in the polarization could affect the direction-finding measurements and produce effects of this type. However, polarization effects are least important in the direction-finding analysis when the source location is near the spin plane of the antenna. For the IMP 8 measurements the source is usually very near the spin plane, which minimizes errors of this type.

Although irregularities in the solar wind density or polarization effects may cause the systematic drift in the direction of arrival of radiation from a type III event at one frequency, there is currently no completely adequate explanation of the drift in source position. Although the changes in the direction of arrival could be caused by a combination of fundamental and second harmonic emission there is still no direct evidence that emission occurs at both frequencies. The effects of changes in the source position are thought to be reduced in this study since the source locations are averaged over the duration of the event. However, the explanation of the drift may provide important insight into the type III emission processes in the solar wind and should be studied in detail.

The results of the analysis presented in this paper are model dependent. It is necessary to use a density scale to determine the heliocentric radial distance at which the radiation is generated. The requirement to assume a density model can be eliminated if the source position is determined by triangulation. For example, simultaneous direction-finding measurements from three spacecraft, two located near the earth to establish the earth-source line and one

located far from the earth to determine the source position along the line, can provide measurements of this type. We hope that simultaneous radio direction-finding measurements from the HELIOS 1 and 2 spacecraft, which are now in orbit around the sun, and from the IMP 8 and HAWKEYE 1 satellites near the earth will be able to provide such measurements. If successful, these multi-spacecraft direction-finding measurements will make it possible to study the three-dimensional structure of the magnetic field in the solar wind completely independent of any modeling assumptions.

ACKNOWLEDGMENTS

The authors thank Dr. M. Montgomery for providing the solar wind density measurements from IMP 8. The authors wish to express their gratitude to Drs. C. K. Goertz and R. R. Shaw for their invaluable comments on this paper.

This work was supported in part by the National Aeronautics and Space Administration under Contracts NAS1-13129 and NAS5-11431 and Grant NGL-16-001-043 and by the Office of Naval Research under Grant N00014-76-C-0016.

REFERENCES

Alexander, J. K., Malitson, H. H., and Stone, R. G.: 1969, "Type III Radio bursts in the outer corona", Solar Phys. 8, 388-397.

Alvarez, H., Haddock, F. T., and Lin, R. P.: 1972, "Evidence for electron excitation of type III radio burst emission", Solar Phys. 26, 468-473.

Alvarez, H., Lin, R. P., and Bame, S. J.: 1975, "Fast solar electrons, interplanetary plasma and KM-wave type III radio bursts observed from the IMP-6 spacecraft", Solar Phys. 44, 485-501.

Coleman, P. J., Jr. and Rosenberg, R. L.: 1971, "The north-south component of the interplanetary magnetic field", J. Geophys. Res. 76, 2917-2926.

Fainberg, J., Evans, L. G., and Stone, R. G.: 1972, "Radio tracking of solar energetic particles through interplanetary space", Science 178, 743-745.

Fainberg, J. and Stone R. G.: 1970, "Type III solar radio burst storms observed at low frequencies (Part II Average excited speed)", Solar Phys. 15, 433-445.

Fainberg, J. and Stone, R. G.: 1971, "Type III solar radio burst storms observed at low frequencies (Part III Streamer density, inhomogeneities and solar wind speed)", Solar Phys. 17, 392-401.

Fainberg, J. and Stone, R. G.: 1974, "Satellite observations of type III solar radio bursts at low frequencies", Space Sci. Rev. 16, 145-188.

Frank, L. A. and Gurnett, D. A.: 1972, "Direct observations of low-energy solar electrons associated with a type III solar radio burst", Solar Phys. 27, 446-465.

Ginzburg, V. L. and Zhelezniakov, V. V.: 1958, "On the possible mechanisms of sporadic solar radio emission (radiation in an isotropic plasma)", Sov. Astron. AJ2, 653-668.

Gurnett, D. A. and Frank, L. A.: 1975, "Electron plasma oscillations associated with type III radio emissions and solar electrons", accepted for publication, Solar Physics.

Haddock, F. T. and Alvarez, H.: 1973, "The prevalence of second harmonic radiation in type III bursts observed at kilometric wavelengths", Solar Phys. 29, 183-196.

Haddock, F. T. and Graedel, T. E.: 1970, "Dynamic spectra of type III solar bursts from 4 to 2 MHz observed by OGO-III", Astrophys. J. 160, 293-300.

Hartz, T. R.: 1964, "Solar noise observations from the Alouette satellite", Ann. Astrophys. 27, 831-836.

Hartz, T. R.: 1969, "Type III solar radio noise bursts at hectometer wavelengths", Planet. Space Sci. 17, 267-287.

Kaiser, M. L.: 1975, "The solar elongation distribution of low frequency radio bursts", Goddard Space Flight Center preprint X-693-75-99.

Kundu, M. R.: 1965, Solar Radio Astronomy, Interscience, New York.

Lin, R. P.: 1970, "The emission and propagation of ~ 40 keV solar flare electrons", Solar Phys. 12, 266-303.

Lin, R. P.: 1974, "Non-relativistic solar electrons", Space Sci. Rev. 16, 189-256.

Lin, R. P., Evans, L. G., and Fainberg, J.: 1973, "Simultaneous observations of fast solar electrons and type III radio burst emission near 1 AU", Astrophys. Lett. 14, 191-198.

Newkirk, G., Jr.: 1967, "Structure of the solar corona", Ann. Rev. Astron. Astrophys. 5, 213-266.

NOAA: December 1974, Solar-Geophysical Data 364, Part II.

NOAA: January 1975, Solar-Geophysical Data 365, Part II.

Parker, E. N.: 1963, Interplanetary Dynamical Processes, Interscience, New York.

Parker, E. N.: 1964, "The penetration of galactic cosmic rays into the solar system", The Solar Wind, Pergamon Press, Oxford.

Parker, E. N.: 1965, "Dynamical theory of the solar wind", Space Sci. Rev. 4, 666-708.

Rosenberg, R. L. and Winge, C. R., Jr.: 1974, "The latitude dependencies of the solar wind", Solar Wind Three, Institute of Geophysics and Planetary Physics, UCIA, 300-310.

Schatten, K. H.: 1972, "Large-scale properties of the interplanetary magnetic field, Solar Wind, NASA publication SP-308, 65-92.

Schatten, K. H., Ness, N. F., and Wilcox, J. M.: 1968, "Influence of a solar active region on the interplanetary magnetic field", Solar Phys. 5, 240-256.

Slysh, V. I.: 1967, "Long-wavelength solar radio emissions observed by the lunar satellites Luna 11 and Luna 12", Cosmic Research (English transl.) 5, 759-769.

Smith, D. F.: 1970, "Type III solar radio bursts", Adv. Astron. Astrophys. 7, 147-226.

Smith, D. F.: 1974, "Type III radio bursts and their interpretation", Space Sci. Rev. 16, 91-144.

Stone, R. G.: 1974, "Traveling solar radio bursts", Solar Wind Three, Institute of Geophys. and Planetary Phys., UCIA, 72-97.

Suess, S. T.: 1974, "Three dimensional modeling, Solar Wind Three, Institute of Geophys. and Planetary Phys., UCIA, 311-317.

Suess, S. T., Hundhausen, A. F., and Pizzo, V.: 1975, "Latitude dependent nonlinear high-speed solar wind streams", J. Geophys. Res. 80, 2023-2029.

Suess, S. T. and Nerney, S. F.: 1975, "The global solar wind and predictions for Pioneers 10 and 11", Geophys. Res. Lett. 2, 75-77.

Van Allen, J. A. and Krimigis, S. M.: 1965, "Impulsive emission of ~ 40 keV electrons from the sun", J. Geophys. Res. 70, 5737-5751.

Wild, J. P.: 1950, "Observations of the spectrum of high-intensity solar radiation at metre wavelengths (III. Isolated bursts)", Aust. J. Sci. Res. A3, 541-557.

Wild, J. P. and McCready, L. L.: 1950, "Observations of the spectrum of high-intensity solar radiation at metre wavelengths (I. The apparatus and spectral types of solar bursts observed)", Aust. J. Sci. Res. A3, 387-398.

Wild, J. P., Murray, J. D., and Rowe, W. C.: 1954, "Harmonics in the spectra of solar radio disturbances", Aust. J. Phys. 7, 439-459.

Wild, J. P., Sheridan, K. V., and Neylan, A. A.: 1959, "An investigation of the speed of the solar disturbances responsible for type III radio bursts", Aust. J. Phys. 12, 369-398.

Table I

Latitude and Longitude of Type III Radio Bursts

(Geocentric Solar Ecliptic Coordinates)

Frequency	Latitude	Longitude
	June 8, 1974	
500 kHz	--	- 7° ±1°
178 kHz	--	-16° ±1°
100 kHz	-24° ± 6°	-20° ±1°
56.2 kHz	-11° ± 7°	9° ±1°
42.2 kHz	-10° ± 9°*	--
31.1 kHz	-32° ±32°*	--
	July 5, 1974	
178 kHz	-21° ± 7°	- 2° ±1°
100 kHz	-20° ± 2°	15° ±6°
56.2 kHz	-30° ±16°*	--
42.2 kHz	-32° ±25°*	--
	July 6, 1974	
500 kHz	--	- 5° ±1
178 kHz	--	- 8° ±1°
100 kHz	--	4° ±1°
56.2 kHz	-31° ± 8°*	--
42.2 kHz	-25° ±15°*	--
31.1 kHz	-11° ±15°*	--

*Involves model fitting, not a direct measurement.

FIGURE CAPTIONS

Figure 1 The position of the source plane relative to the satellite spin axis, null position (δ), and the sun for HAWKEYE 1 and IMP 8. The vector $\hat{n}$ is perpendicular to the source plane, and the spin axis ($\vec{S}$) is perpendicular to the spin plane. The source planes for IMP 8 and HAWKEYE 1 intersect, and the source is located along this intersection. The source location is computed by taking the cross product between $\hat{n}_1$, a vector normal to the IMP 8 source plane, and $\hat{n}_2$, a vector normal to the HAWKEYE 1 source plane. θ is the angle between the spin axis of the satellite and the sun-satellite line.

Figure 2 A type III burst observed simultaneously by HAWKEYE 1 and IMP 8. The type III burst is characterized by a rapid decrease in frequency with increasing time, and at each frequency the intensity has a rapid rise time followed by a slower exponential decay.

Figure 3 The amplitude, geocentric solar ecliptic longitude, and modulation factor for a type III burst detected by IMP 8 on June 21 at 100 kHz. The spin modulation is evident as a small amplitude, periodic change in the observed intensity. The longitude drifts from near zero degrees near the begin-

ing of the event to about 45° near the end. The modulation factor near the beginning of the event averages about 0.65, dropping to about 0.25 at the end of the event. The apparent shift in source location could be caused by polarization effects, density inhomogeneities, or by radiation from different source regions at both the fundamental and second harmonic of the plasma frequency.

Figure 4 The RAE emission level scale gives the average radial distance of a type III burst from the sun as a function of frequency of emission. The density scale assumes emission at the second harmonic of the plasma frequency. For one of the events analyzed the RAE emission level scale was adjusted so that the density at 1.0 AU agreed with *in situ* measurements at 1.0 AU.

Figure 5 Three models of the solar magnetic field.
Constant Latitude: Archimedean spirals wound on cones of constant heliocentric latitude.
Convergent field line model: Archimedean spiral field lines which extend to lower heliocentric latitude with increasing radial distance.
Divergent field line model: Archimedean spiral field lines which extend to higher heliocentric latitudes with increasing radial distance.

Figure 6 Source locations for a type III event (June 8). The source locations follow an Archimedean spiral configuration in the ecliptic plane. The source locations out of the ecliptic are shown as a function of heliocentric latitude and radial distance. The bottom panels show the geocentric longitude and latitude of the source predicted by a least squares fit of the constant latitude field line model to the observed geocentric longitudes and latitudes. Note that this event deviates from the constant latitude model at 56.2 kHz and 42.2 kHz implying that the magnetic field lines may extend to lower heliographic latitudes with increasing radial distance. The predicted flare location is found by extrapolating the least squares fit field line back to the sun.

Figure 7 Direction-finding measurements for another type III event (July 5). Projected into the ecliptic plane the source locations follow an Archimedean spiral configuration. Out of the ecliptic plane the source locations are at nearly constant heliocentric latitudes. Except for the 100 kHz emission the data is consistent with the constant latitude model.

Figure 8 Direction-finding measurements for the third type III event (July 6). Projected into the ecliptic plane the source regions follow an Archimedean spiral configuration. Out of the ecliptic the source locations are at very nearly constant latitude, which is in excellent agreement with the constant latitude model for the solar magnetic field.

Figure 9 The source size of a type III burst as a function of frequency as seen from the earth using a thin, flat disk as the modeled source. As the source region approaches the earth the source size increases, as would be expected.

Figure 10 Source sizes as a function of frequency for the same event as in Figure 9 viewed from the sun. Note that the source size remains essentially constant in the range from 500 to 100 kHz. The source sizes are, however, larger than those previously determined from particle measurements.

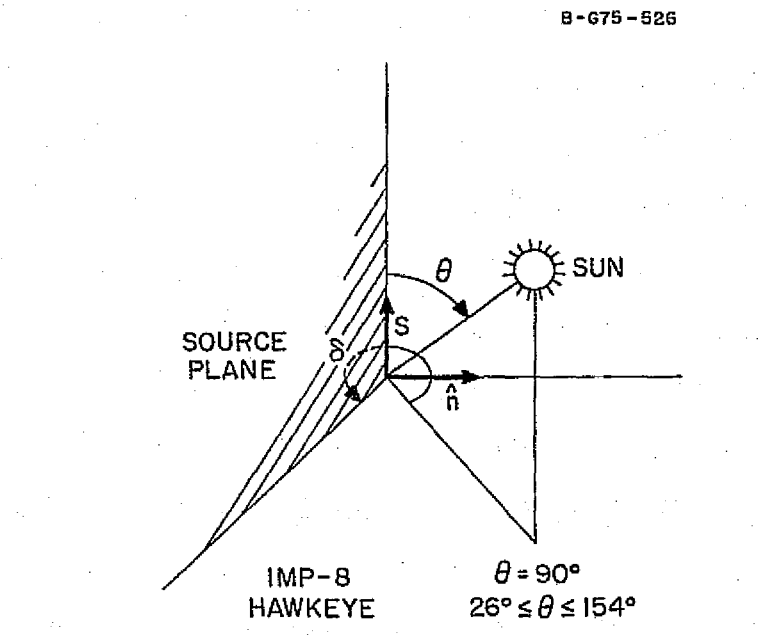
B-G75-526
θ
SUN
S
δ
SOURCE
PLANE
n̂
IMP-8
HAWKEYE
θ = 90°
26° ≤ θ ≤ 154°

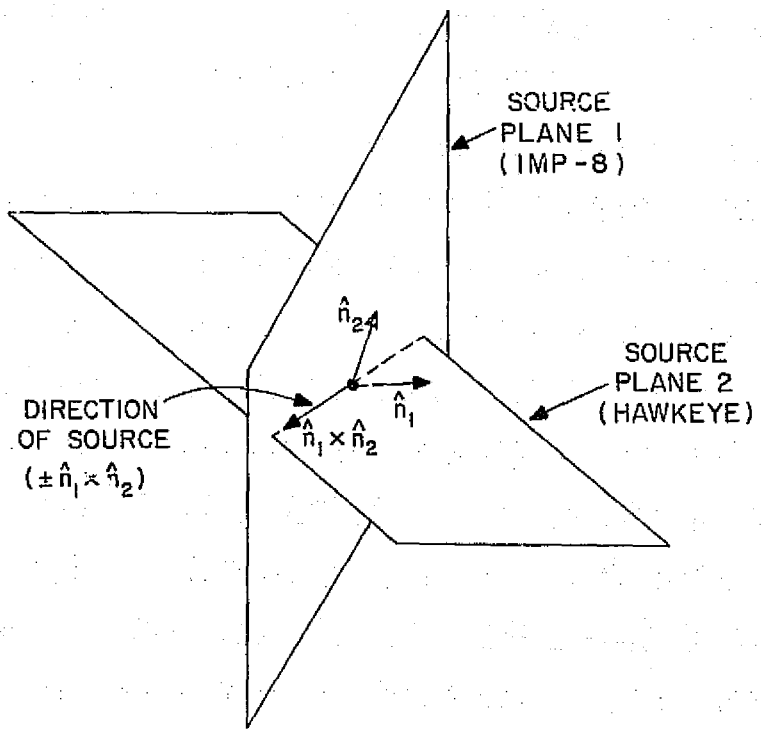
SOURCE
PLANE 1
(IMP-8)
n̂24
SOURCE
PLANE 2
(HAWKEYE)
DIRECTION
OF SOURCE
(± n̂1 × n̂2)
n̂1
n̂1 × n̂2

Figure 1

C-G75-781-I

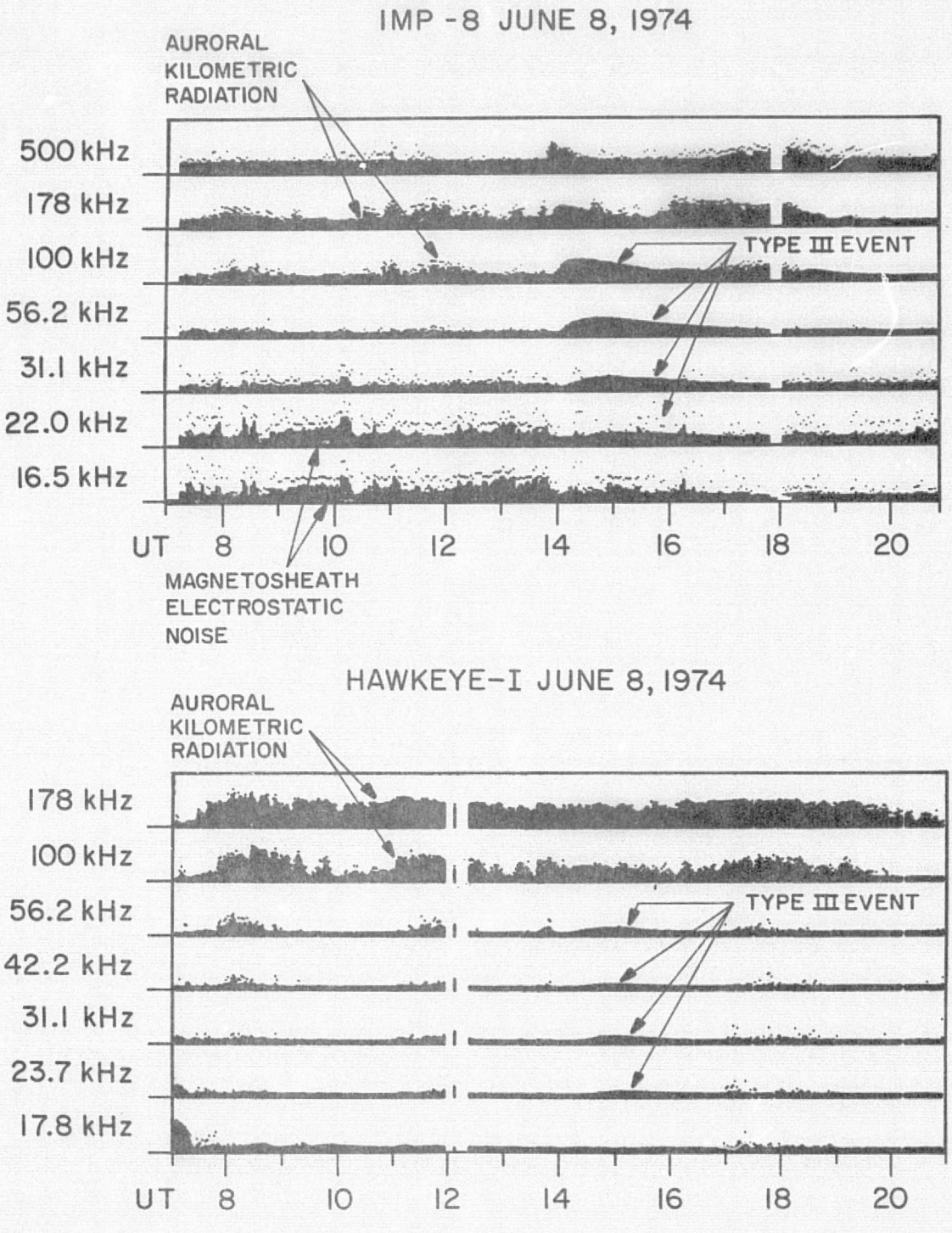

Figure 2

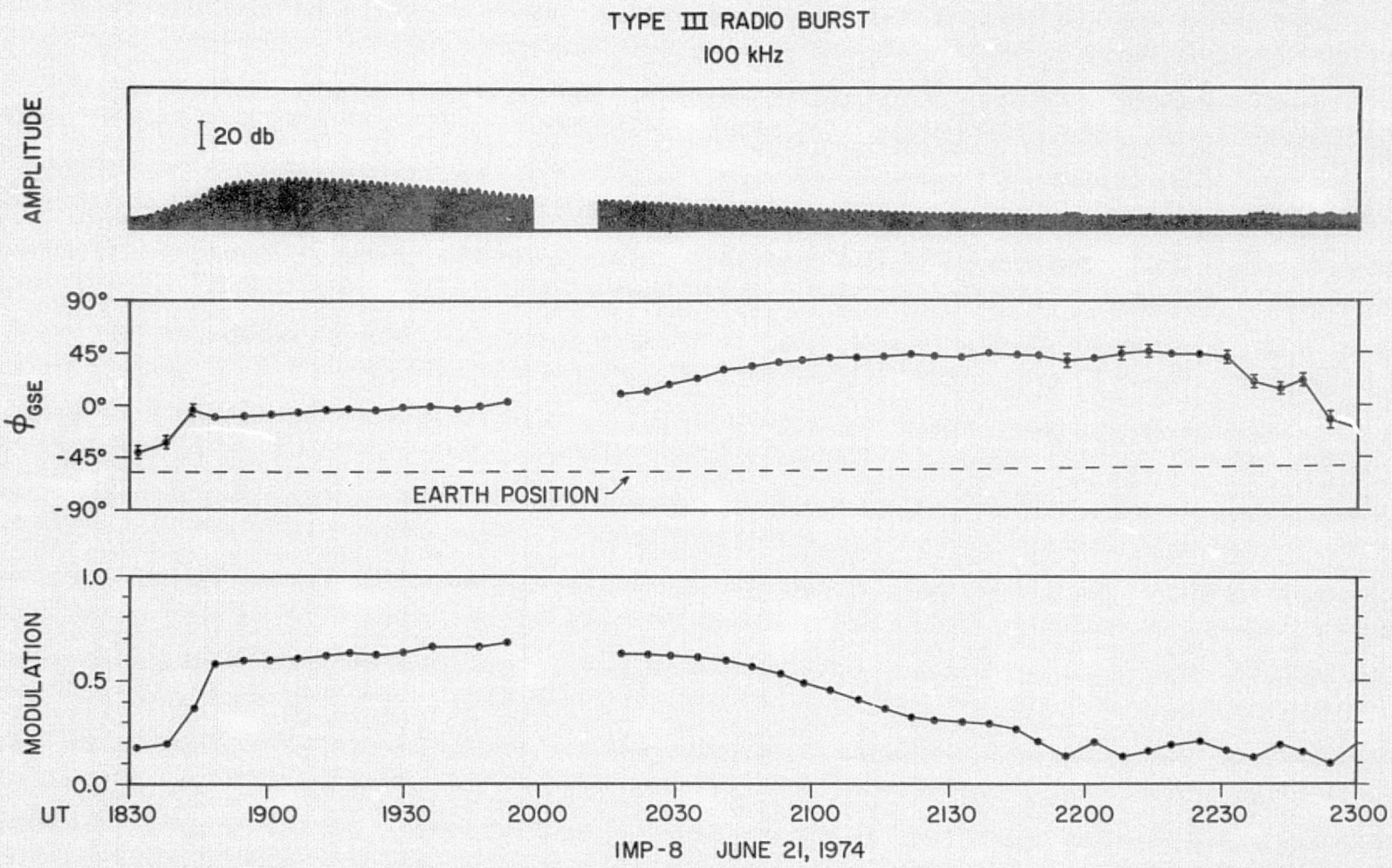
TYPE III RADIO BURST
100 kHz
AMPLITUDE
20 db
90°
45°
0°
-45°
-90°
ϕ_{GSE}
EARTH POSITION
1.0
0.5
0.0
MODULATION
UT
1830
1900
1930
2000
2030
2100
2130
2200
2230
2300
IMP-8 JUNE 21, 1974

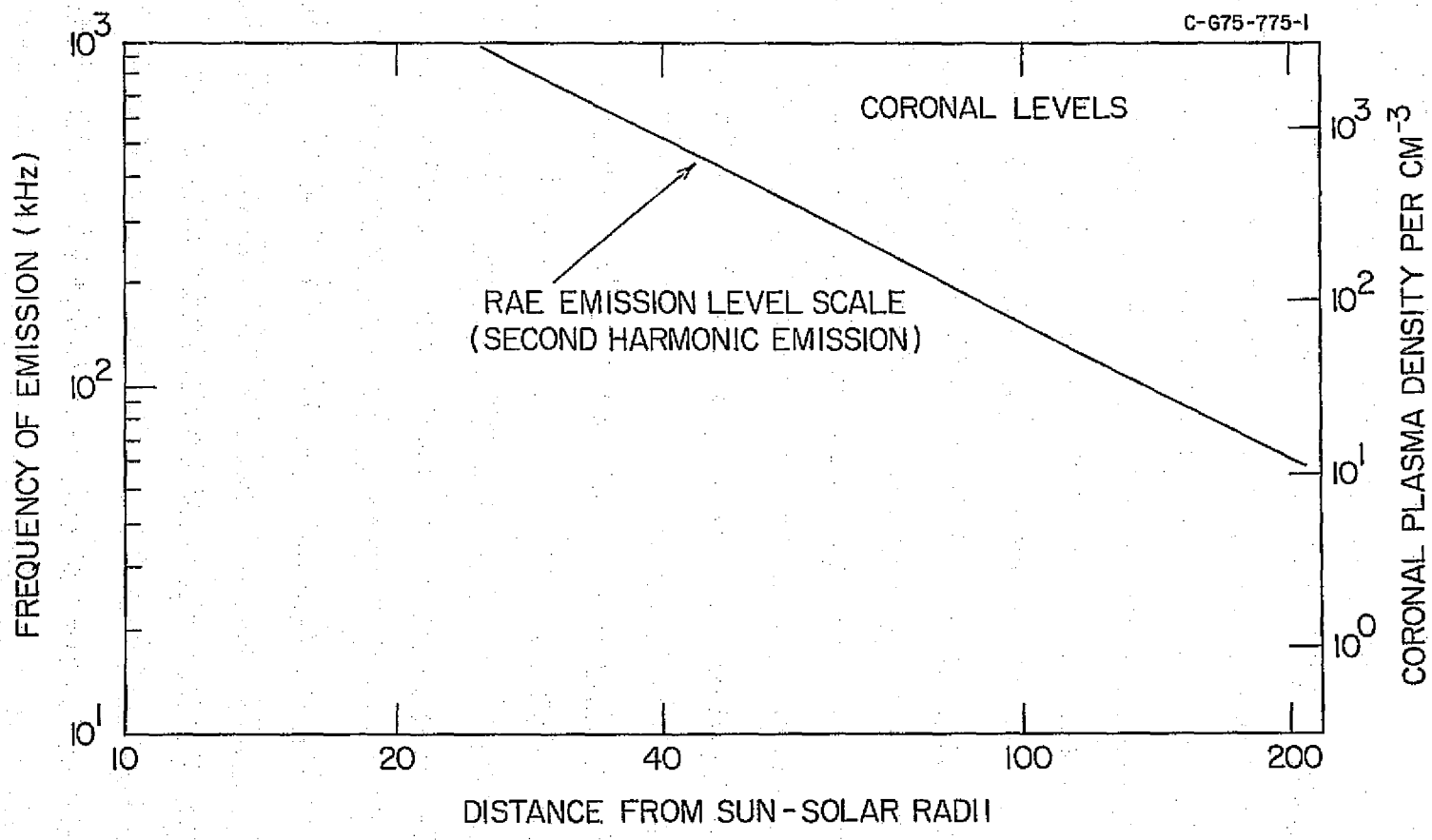
C-G75-775-I
CORONAL LEVELS
RAE EMISSION LEVEL SCALE
(SECOND HARMONIC EMISSION)
FREQUENCY OF EMISSION (kHz)
10^3
10^2
10^1
10
20
40
100
200
DISTANCE FROM SUN - SOLAR RADII
CORONAL PLASMA DENSITY PER CM^{-3}
10^3
10^2
10^1
10^0

Figure 4

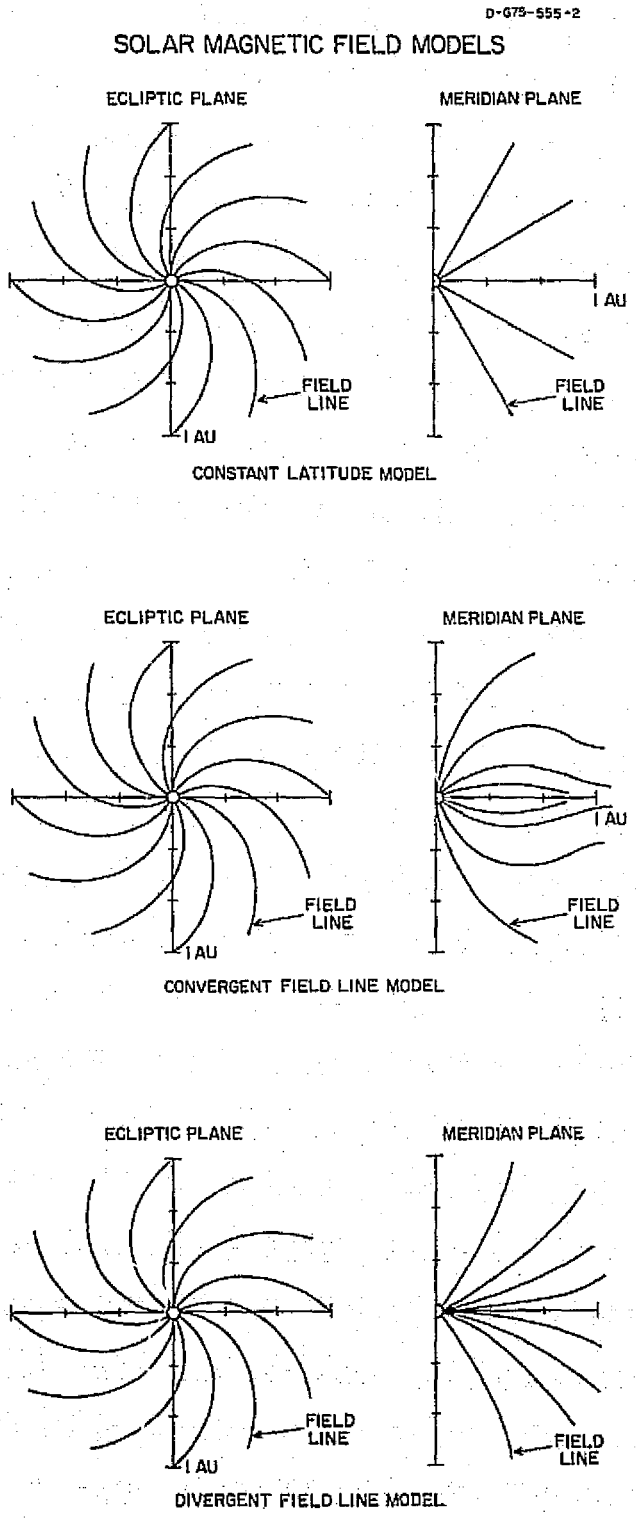
D-G75-555-2
SOLAR MAGNETIC FIELD MODELS
ECLIPTIC PLANE
MERIDIAN PLANE
1 AU
FIELD LINE
1 AU
FIELD LINE
CONSTANT LATITUDE MODEL
ECLIPTIC PLANE
MERIDIAN PLANE
1 AU
FIELD LINE
1 AU
FIELD LINE
CONVERGENT FIELD LINE MODEL
ECLIPTIC PLANE
MERIDIAN PLANE
FIELD LINE
1 AU
FIELD LINE
DIVERGENT FIELD LINE MODEL

Figure 5

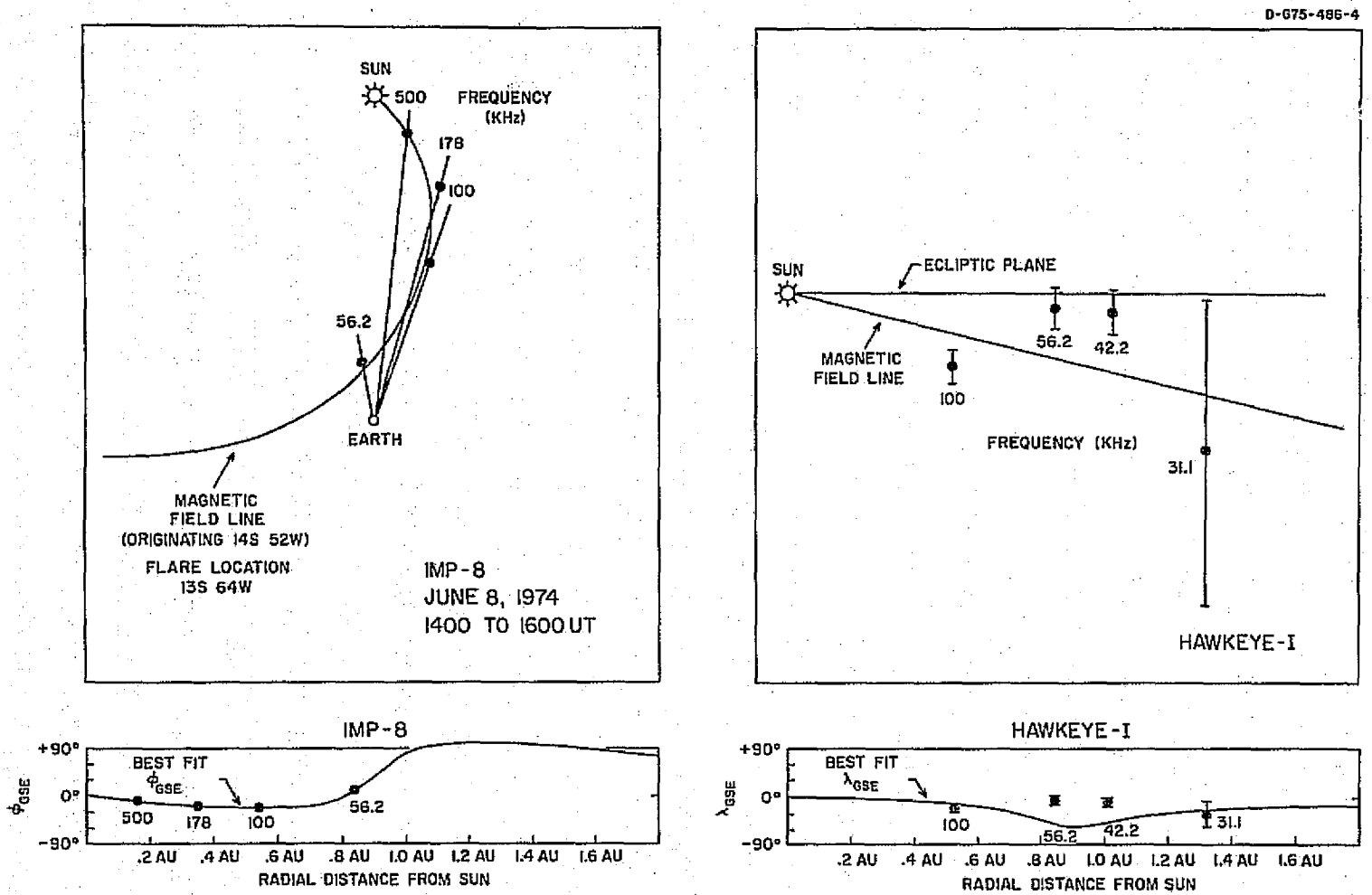
D-G75-486-4
SUN
500
FREQUENCY (KHz)
178
100
56.2
EARTH
MAGNETIC FIELD LINE (ORIGINATING 14S 52W)
FLARE LOCATION 13S 64W
IMP-8
JUNE 8, 1974
1400 TO 1600 UT
SUN
ECLIPTIC PLANE
56.2
42.2
MAGNETIC FIELD LINE
100
FREQUENCY (KHz)
31.1
HAWKEYE-I
IMP-8
+90°
0°
-90°
BEST FIT
ϕ_{GSE}
500
178
100
56.2
.2 AU
.4 AU
.6 AU
.8 AU
1.0 AU
1.2 AU
1.4 AU
1.6 AU
RADIAL DISTANCE FROM SUN
HAWKEYE-I
+90°
0°
-90°
BEST FIT
λ_{GSE}
100
56.2
42.2
31.1
.2 AU
.4 AU
.6 AU
.8 AU
1.0 AU
1.2 AU
1.4 AU
1.6 AU
RADIAL DISTANCE FROM SUN

Figure 6

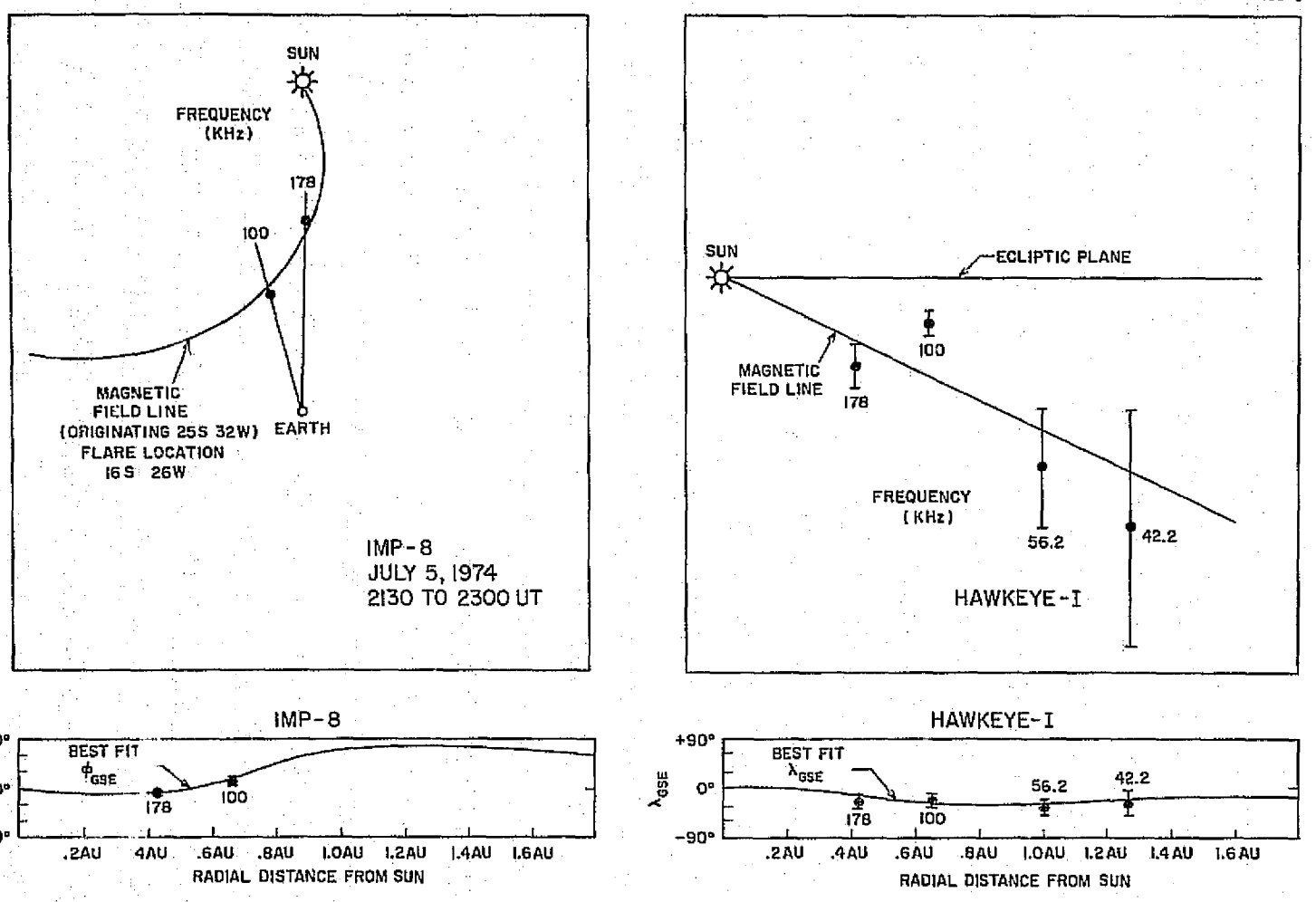
SUN
FREQUENCY
(KHz)
178
100
MAGNETIC
FIELD LINE
(ORIGINATING 25S 32W)
FLARE LOCATION
16S 26W
EARTH
IMP-8
JULY 5, 1974
2130 TO 2300 UT
SUN
ECLIPTIC PLANE
MAGNETIC
FIELD LINE
100
178
FREQUENCY
(KHz)
56.2
42.2
HAWKEYE-I
IMP-8
+90°
0°
-90°
BEST FIT
ϕ_{GSE}
178
100
.2AU
.4AU
.6AU
.8AU
1.0AU
1.2AU
1.4AU
1.6AU
RADIAL DISTANCE FROM SUN
HAWKEYE-I
+90°
0°
-90°
BEST FIT
λ_{GSE}
178
100
56.2
42.2
.2AU
.4AU
.6AU
.8AU
1.0AU
1.2AU
1.4AU
1.6AU
RADIAL DISTANCE FROM SUN

Figure 7

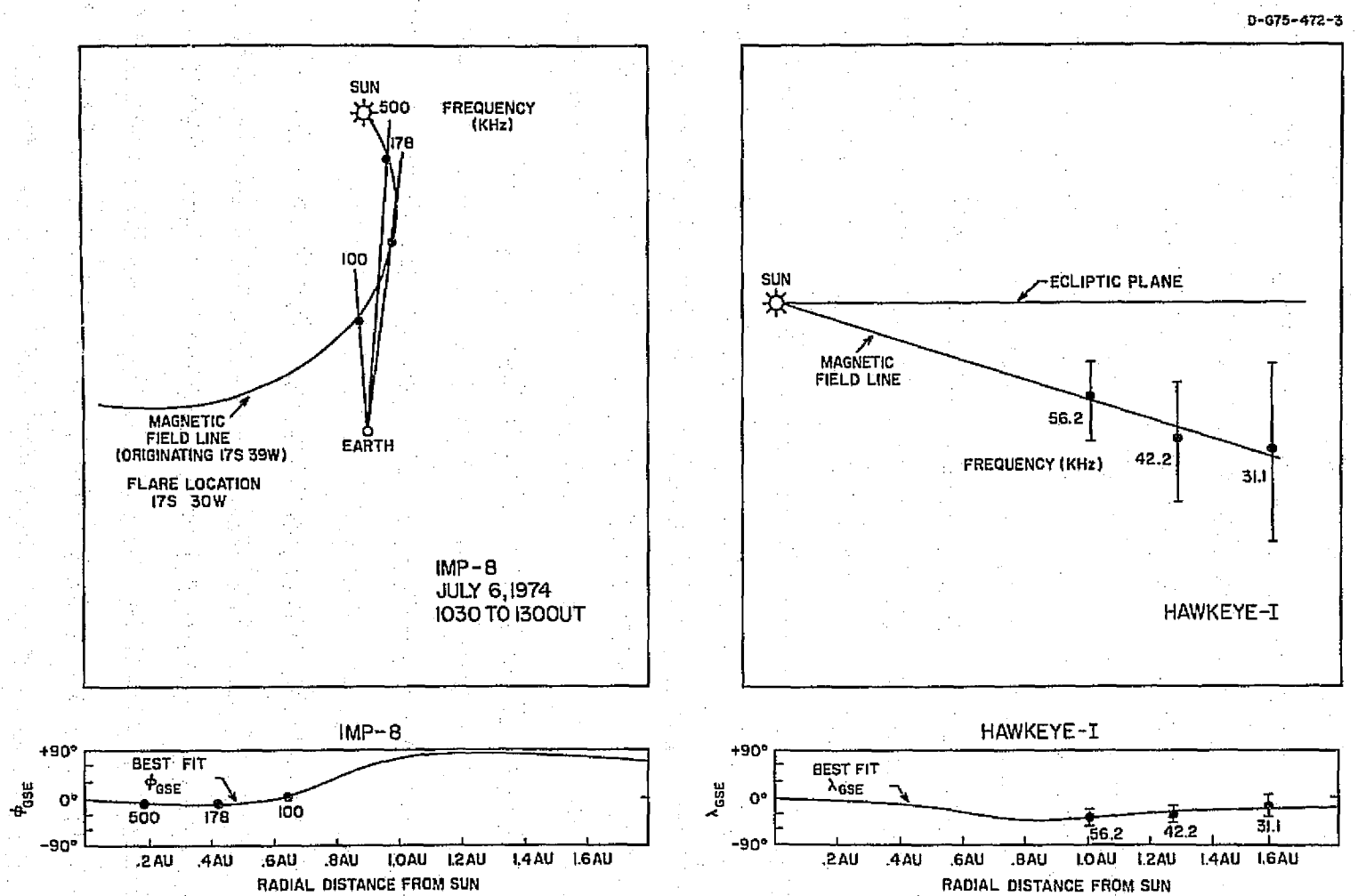
D-G75-472-3
SUN
500
FREQUENCY (KHz)
178
100
MAGNETIC FIELD LINE (ORIGINATING 17S 39W)
FLARE LOCATION 17S 30W
EARTH
IMP-8
JULY 6, 1974
1030 TO 1300UT
SUN
ECLIPTIC PLANE
MAGNETIC FIELD LINE
56.2
42.2
31.1
FREQUENCY (KHz)
HAWKEYE-I
IMP-8
+90°
0°
-90°
ϕ_{GSE}
BEST FIT ϕ_{GSE}
500
178
100
.2AU .4AU .6AU .8AU 1.0AU 1.2AU 1.4AU 1.6AU
RADIAL DISTANCE FROM SUN
HAWKEYE-I
+90°
0°
-90°
λ_{GSE}
BEST FIT λ_{GSE}
56.2
42.2
31.1
.2AU .4AU .6AU .8AU 1.0AU 1.2AU 1.4AU 1.6AU
RADIAL DISTANCE FROM SUN

Figure 8

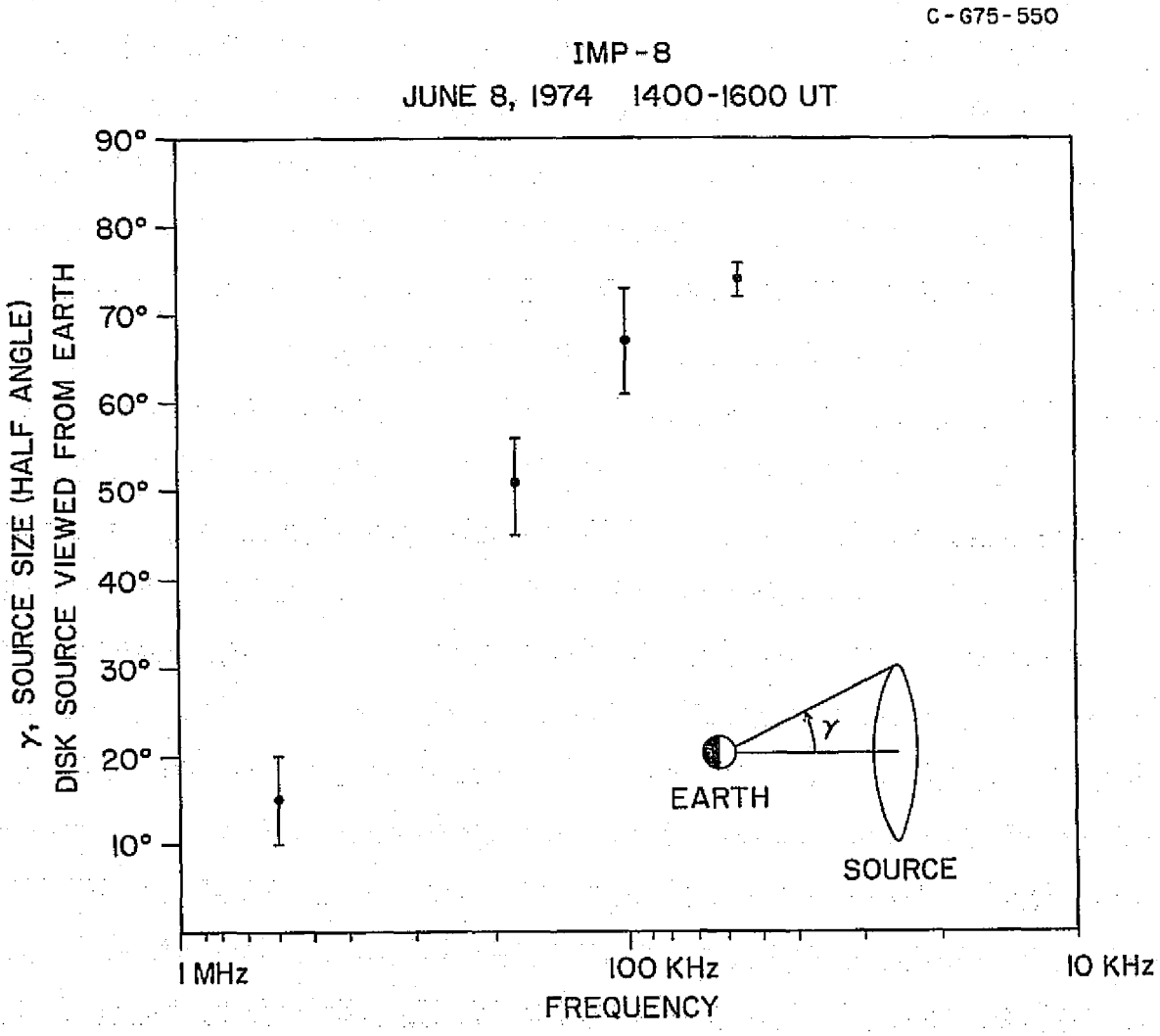
C-675-550
IMP-8
JUNE 8, 1974 1400-1600 UT
γ, SOURCE SIZE (HALF ANGLE)
DISK SOURCE VIEWED FROM EARTH
90°
80°
70°
60°
50°
40°
30°
20°
10°
γ
EARTH
SOURCE
1 MHz
100 KHz
10 KHz
FREQUENCY

Figure 9

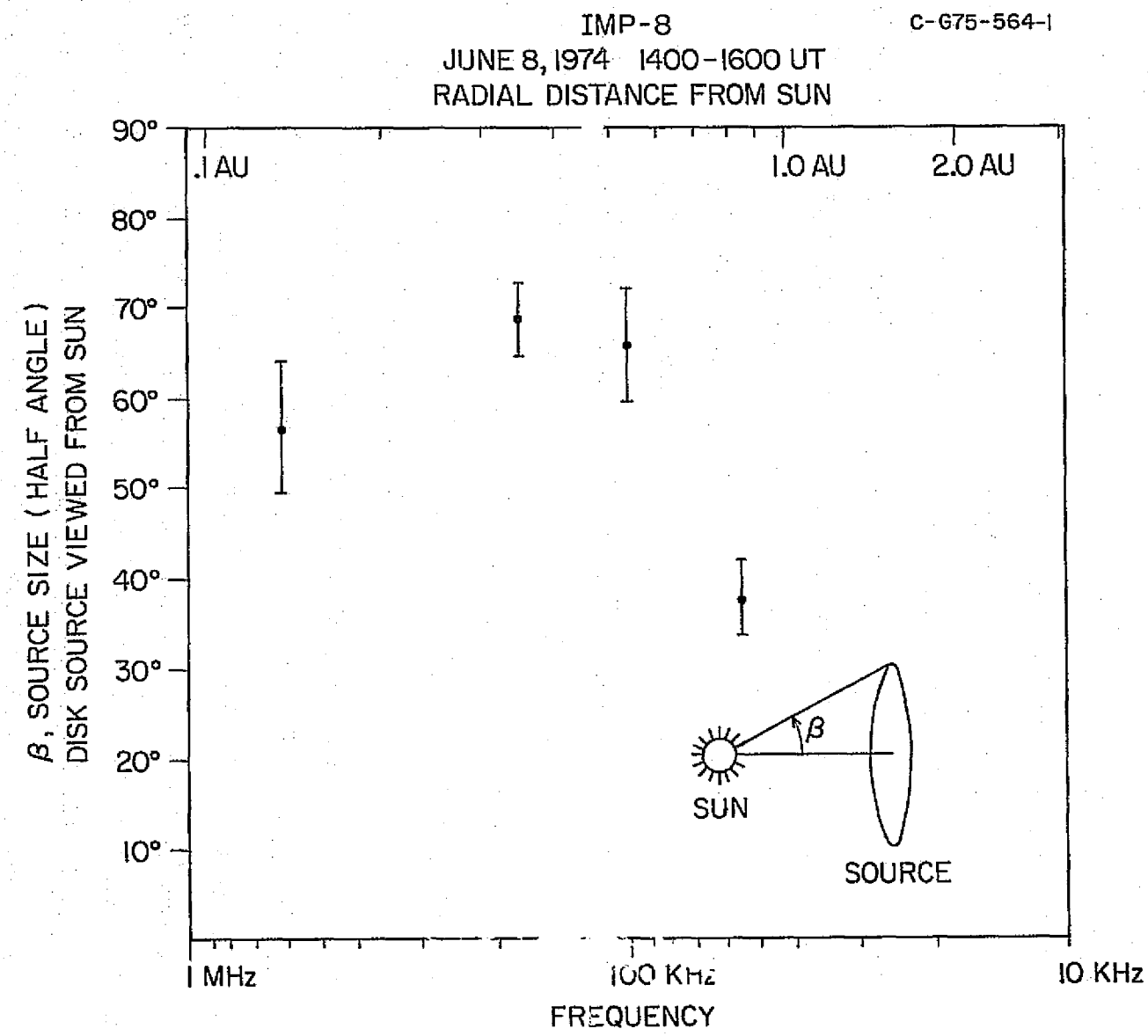
IMP-8
JUNE 8, 1974 1400-1600 UT
RADIAL DISTANCE FROM SUN
C-G75-564-1
90°
80°
70°
60°
50°
40°
30°
20°
10°
.1 AU
1.0 AU
2.0 AU
β, SOURCE SIZE (HALF ANGLE)
DISK SOURCE VIEWED FROM SUN
β
SUN
SOURCE
1 MHz
100 KHz
10 KHz
FREQUENCY

Figure 10